

# Ablation of AMP-activated protein kinase $\alpha 1$ and $\alpha 2$ from mouse pancreatic beta cells and *RIP2.Cre* neurons suppresses insulin release in vivo

G. Sun · A. I. Tarasov · J. McGinty · A. McDonald · G. da Silva Xavier · T. Gorman · A. Marley · P. M. French · H. Parker · F. Gribble · F. Reimann · O. Prendiville · R. Carzaniga · B. Viollet · I. Leclerc · G. A. Rutter

Received: 19 November 2009 / Accepted: 1 February 2010 / Published online: 11 March 2010  
© Springer-Verlag 2010

## Abstract

**Aims/hypothesis** AMP-activated protein kinase (AMPK) is an evolutionarily conserved enzyme and a target of glucose-lowering agents, including metformin. However, the precise role or roles of the enzyme in controlling insulin secretion remain uncertain.

**Methods** The catalytic  $\alpha 1$  and  $\alpha 2$  subunits of AMPK were ablated selectively in mouse pancreatic beta cells and hypothalamic neurons by breeding *Ampk $\alpha 1$*  [also known as *Prkaa1*]-knockout mice, bearing floxed *Ampk $\alpha 2$*  [also known as *Prkaa2*] alleles (*Ampk $\alpha 1$ <sup>-/-</sup>, $\alpha 2$ <sup>fl/fl</sup>*), with mice expressing *Cre* recombinase under the rat insulin promoter (*RIP2*). *RIP2* was used to express constitutively activated AMPK selectively in beta cells in transgenic mice. Food intake, body weight and urinary catecholamines were

measured using metabolic cages. Glucose and insulin tolerance were determined after intraperitoneal injection. Beta cell mass and morphology were analysed by optical projection tomography and confocal immunofluorescence microscopy, respectively. Granule docking, insulin secretion, membrane potential and intracellular free  $\text{Ca}^{2+}$  were measured with standard techniques.

**Results** Trigenic *Ampk $\alpha 1$ <sup>-/-</sup>, $\alpha 2$ <sup>fl/fl</sup>* expressing *Cre* recombinase and lacking both AMPK $\alpha$  subunits in the beta cell, displayed normal body weight and increased insulin sensitivity, but were profoundly insulin-deficient. Secreted catecholamine levels were unchanged. Total beta cell mass was unaltered, while mean islet and beta cell volume were reduced. AMPK-deficient beta cells displayed normal glucose-induced changes in membrane potential and intracel-

**Electronic supplementary material** The online version of this article (doi:10.1007/s00125-010-1692-1) contains supplementary material, which is available to authorised users.

G. Sun · A. I. Tarasov · A. McDonald · G. da Silva Xavier · I. Leclerc (✉) · G. A. Rutter (✉)  
Section of Cell Biology, Division of Diabetes, Endocrinology and Metabolism, Department of Medicine, Faculty of Medicine, Imperial College London, Sir Alexander Fleming Building, Exhibition Road, South Kensington, London SW7 2AZ, UK  
e-mail: i.leclerc@imperial.ac.uk  
e-mail: g.rutter@imperial.ac.uk

J. McGinty · P. M. French  
Photonics Group, Department of Physics, Imperial College London, London, UK

T. Gorman · A. Marley  
AstraZeneca, Alderley Edge, UK

H. Parker · F. Gribble · F. Reimann  
Cambridge Institute of Medical Research, Cambridge, UK

O. Prendiville  
Charing Cross Hospital, Imperial College London, London, UK

R. Carzaniga  
Electron Microscopy Centre, Imperial College London, London, UK

B. Viollet  
Institut Cochin, Université Paris Descartes, CNRS (UMR 8104), Paris, France

B. Viollet  
Inserm, U1067 Paris, France

lular free  $\text{Ca}^{2+}$ , while granule docking and insulin secretion were enhanced. Conversely,  $\beta$ AMPK transgenic mice were glucose-intolerant and displayed defective insulin secretion. **Conclusions/interpretation** Inhibition of AMPK activity within the beta cell is necessary, but not sufficient for stimulation of insulin secretion by glucose to occur. AMPK activation in extrapancreatic *RIP2.Cre*-expressing cells might also influence insulin secretion in vivo.

**Keywords** AMPK · Beta cell · Insulin secretion · Islet · Knockout · RIP.Cre

### Abbreviations

AICAR	5-Aminoimidazole-4-carboxamide ribonucleotide
AMPK	AMP-activated protein kinase
AMPK.CA	AMPK $\alpha$ 1 <sup>S12.T172D</sup>
$\beta$ AMPKdKO	<i>Ampk<math>\alpha</math>1</i> <sup>-/-</sup> , <i><math>\alpha</math>2</i> <sup>fl/fl</sup> mice expressing <i>Cre</i> recombinase ( <i>Ampk<math>\alpha</math>1</i> <sup>-/-</sup> , <i><math>\alpha</math>2</i> <sup>fl/fl</sup> , <i>Cre</i> <sup>+</sup> )
AMPK.DN	AMPK $\alpha$ 2.D157A
K <sub>ATP</sub>	ATP-sensitive K <sup>+</sup>
LKB1	Liver kinase B1
mTOR	Mechanistic target of rapamycin
RIP	Rat insulin promoter
ZO-1	Zona occludins-1

### Introduction

AMP-activated protein kinase (AMPK) is an evolutionarily conserved fuel-sensitive protein kinase implicated in the control of glucose homeostasis and playing roles in insulin-sensitive tissues [1–3] and in the pancreatic beta cell [4–7]. While the stimulation of AMPK activity in muscle and liver is now seen as a likely mechanism through which glucose-lowering agents, including metformin and thiazolidinediones, act to improve insulin sensitivity [8], the long-term effects of these agents on pancreatic beta cell survival and insulin release are less clear [7].

Mammalian AMPK is a trimeric protein comprising a catalytic  $\alpha$ -subunit, encoded by one of two separate genes (*Ampk $\alpha$ 1* [also known as *Prkaa1*] and *Ampk $\alpha$ 2* [also known as *Prkaa2*]), a scaffold  $\beta$ - ( $\beta$ 1 or  $\beta$ 2) subunit and a regulatory  $\gamma$ -subunit ( $\gamma$ 1,  $\gamma$ 2 or  $\gamma$ 3) [9, 10]. The existence of two separate AMPK $\alpha$  subunit genes has so far hindered investigations of the role AMPK activity plays in controlling glucose homeostasis in mammals, since the unconditional deletion of both isoforms leads to early embryonic lethality in mice [11]. By contrast, animals with global inactivation of the AMPK $\alpha$ 1 isoform do not display significant metabolic abnormalities [11, 12]. Deletion of the *Ampk $\alpha$ 2* gene leads to insulin resistance and glucose intolerance, in part due to

increased parasympathetic tone [13]. Whereas insulin secretion was normal in islets isolated from whole-body *Ampk $\alpha$ 2* knockout mice, insulin release in vivo appeared to be diminished when measured at a single time point during oral glucose tolerance tests. However, no measurements were made during intraperitoneal glucose tolerance tests, where the complicating effects of potentially altered incretin release could be excluded. Importantly, since complexes containing the AMPK $\alpha$ 1 isoform are substantially (>tenfold) more abundant in beta cell lines than AMPK $\alpha$ 2 complexes [5], increases in expression of the former may also, in part, have compensated for the loss of AMPK $\alpha$ 2.

The cell-permeant AMPK activator, 5-aminoimidazole-4-carboxamide ribonucleotide (AICAR), diminishes glucose-stimulated insulin secretion from clonal beta cells and islets [4, 6], an effect mimicked by the biguanide metformin [14] or by the expression of a constitutively active form of AMPK [6]. Moreover, overexpression of constitutively active AMPK diminished the performance of islets transplanted into streptozotocin-induced diabetic mice [15]. These actions may be due in part to blockade of secretory granule transport to the cell surface [16] as a result of kinesin-1 light chain phosphorylation [17]. In addition, AMPK activation decreases beta cell viability [18, 19] possibly by phosphorylating the cell cycle regulator, p53 [20]. By contrast, inhibition of AMPK activity with dominant-negative forms of the enzyme tends to increase insulin secretion at low glucose concentrations [6] without affecting release at elevated glucose concentrations [21], a finding that is consistent with inactivation of the enzyme as a result of AMP depletion under these conditions.

AMPK is also thought to play an important role in the central control of feeding and glucose homeostasis. Thus, forced changes in AMPK in the ventromedial hypothalamus achieved by stereotactic injection of viral vectors led to marked changes in food intake and body weight [22] and in hypoglycaemia sensing [23, 24]. Moreover, the deletion of *Ampk $\alpha$ 2* in neurons expressing pro-opiomelanocortin or agouti-related peptide leads respectively to increased or decreased food intake in mice [25]. Finally, manipulation of AMPK activity ex vivo was found to affect glucose-induced changes in the electrical activity of  $\text{Ca}^{2+}$  transients in isolated agouti-related peptide (glucose-inhibited), but not in pro-opiomelanocortin (glucose-responsive) neurons in culture [26, 27].

We have previously demonstrated distinct roles in the pancreatic beta cell for AMPK complexes containing differing catalytic subunits [5]. Thus, the  $\alpha$ 2 subunit, which displayed substantial nuclear localisation [4, 5], was implicated in control of gene expression, whereas  $\alpha$ 1-containing complexes, whose total activity exceeded that of  $\alpha$ 2-containing complexes by five to ten fold [5], were almost exclusively cytosolic. The role of the latter remains unclear, but may include regulation of plasma membrane

ion channels, as proposed in oxygen-sensing cells in the carotid body [28].

To assess the role of AMPK in insulin-expressing cells, we generated trigenic mice that were globally inactivated for *Ampkα1* and had *Ampkα2* deleted selectively in pancreatic beta cells and in a small population of hypothalamic neurons, using the rat insulin promoter (RIP)2 [29] and transgenic mice expressing activated AMPK selectively in beta cells. Using these models we highlight multiple novel mechanisms through which AMPK controls insulin production and glucose homeostasis in mammals.

## Methods

Generation of mutant mice lacking *Ampkα1* globally and selectively lacking *Ampkα2* in pancreatic beta cells and *RIP2.Cre* neurons

*Ampkα1*<sup>+/-</sup>, *α2*<sup>fl/fl</sup> (*fl/fl*) mice were first crossed with wild-type C57BL/6 mice to generate double heterozygous *Ampkα1*<sup>+/-</sup>, *α2*<sup>fl/+</sup> mice. Offspring were then crossed with heterozygous *RIP2.Cre*<sup>+</sup> transgenic mice (expressing *Cre* recombinase under the RIP2; Jackson Laboratory, Bar Harbor, ME, USA). The resulting triple heterozygous AMPKα1<sup>+/-</sup>, *α2*<sup>fl/+</sup>, *Cre*<sup>+</sup> mice were interbred with their siblings. Since *RIP2.Cre* transgenic mice have been suggested to show glucose intolerance and impaired insulin secretion [30, 31], *Cre*<sup>+</sup> mice were always used as a negative control. Due to the low probability (1:64) of obtaining double knockout mice through heterozygote crossing, two different breeding strategies were used to obtain double AMPK knockout mice and their littermate controls. First, to generate *Ampkα1*-knockout mice, bearing floxed *Ampkα2* alleles (*Ampkα1*<sup>-/-</sup>, *α2*<sup>fl/fl</sup>) and expressing *Cre* recombinase (βAMPKdKO) and their heterozygous *Ampkα1*<sup>+/-</sup>, *α2*<sup>fl/+</sup>, *Cre*<sup>+</sup> mice controls, *Ampkα1*<sup>-/-</sup>, *α2*<sup>fl/+</sup>, *Cre*<sup>-</sup> and *Ampkα1*<sup>+/-</sup>, *α2*<sup>fl/fl</sup>, *Cre*<sup>+</sup> mice were crossed. Second, to produce heterozygous *Ampkα1*<sup>+/-</sup>, *α2*<sup>fl/+</sup>, *Cre*<sup>+</sup> and their wild-type *Ampkα1*<sup>+/+</sup>, *α2*<sup>+/+</sup>, *Cre*<sup>+</sup> littermate controls, *Ampkα1*<sup>+/-</sup>, *α2*<sup>fl/+</sup>, *Cre*<sup>+</sup> and wild-type mice were crossed. All mice were kept on a C57BL/6 background and offspring genotypes were obtained in the expected Mendelian ratios.

Generation of mutant mice selectively overexpressing AMPK.CA or -DN in pancreatic beta cells and *RIP.Cre* neurons

An expression vector containing the RIP2 promoter fragment (600 bp), *c-myc*-tagged rat AMPKα1<sup>312.T172D</sup> (CA) or AMPKα2.D157A (DN) cDNA, and an SV40 poly

(A) cassette was excised with BssHIII and microinjected into the male pronucleus of fertilised C57BL/6 oocytes. The injected zygotes were re-implanted into pseudo-pregnant female C57BL/6 mice (GenOway, Lyon Cedex, France). We obtained three AMPK.CA (named C1, C2 and C10) and two AMPK.DN (D1 and D2) founder mice that stably transferred the corresponding transgenes to their offspring. Founder mice were crossed with wild-type C57BL/6 mice to achieve F1 generation. Distributions of genotypes in the offspring followed a Mendelian pattern. All AMPK transgenic mice were kept heterozygous. F3 and later generations, and their littermate wild-type controls were used for experiments. All lines were maintained on a pure C57BL/6 background.

### Mouse maintenance and diet

Mice were housed two to five animals per cage in a pathogen-free facility with 12 h light/dark cycle and had free access to standard mouse chow diet or a high-fat diet (60% [wt/wt] fat content; Research Diet, New Brunswick, NJ, USA). As indicated, 6-week-old mice were transferred to a high-fat diet for a maximum of 18 weeks. All in vivo procedures described here were performed at the Imperial College Central Biomedical Service and approved by the UK Home Office Animals Scientific Procedures Act, 1986.

### Body weight and food intake

Fed mouse weights were monitored weekly after 6 weeks of age. Food intake was measured daily for three consecutive days using a metabolic cage.

### In vivo physiological studies

**Intraperitoneal glucose tolerance test** Mice fasted for 15 h (water allowed) were intraperitoneally injected with 1 g glucose/kg mouse weight. Blood from the tail vein was obtained at 0, 15, 30, 60, 90 and 120 min after injection. Blood glucose levels were measured with an automatic glucometer (Accucheck; Roche, Burgess Hill, UK). To study the effect of α-adrenergic antagonist on glucose tolerance, mice were intraperitoneally injected with 10 mg/kg mouse weight phentolamine 30 min before glucose challenge.

**Plasma insulin measurement** Mice fasted for 15 h were intraperitoneally injected with 3 g glucose/kg mouse weight. Blood from mice tail veins was collected into a heparin coated tube (Sarstedt, Beaumont Leys, UK) at 0, 15 and 30 min after injection. Plasma was separated by centrifuging the blood at 2,000 g for 5 min. Plasma insulin levels were measured using an ultrasensitive mouse insulin ELISA kit (Mercodia, Uppsala, Sweden). Normal fed plasma insulin levels were

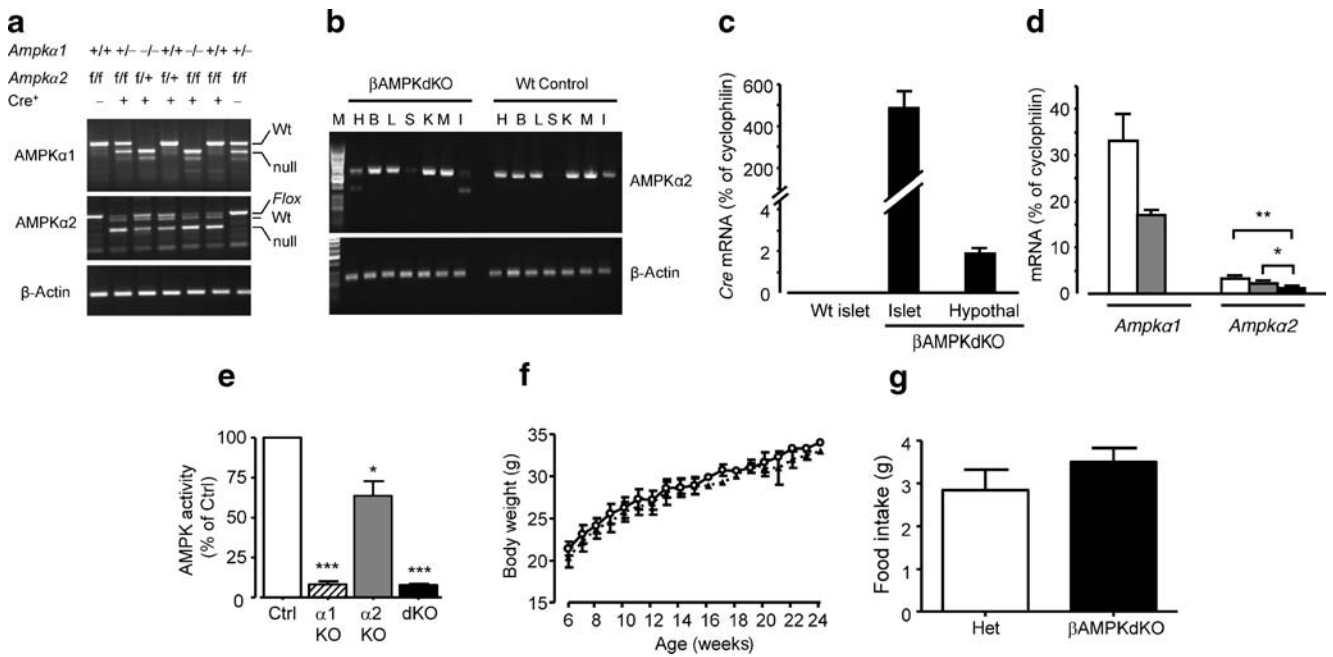


**Fig. 1** Generation of  $\beta$ AMPKdKO mice. **a** RT-PCR analysis of the deletion of AMPK $\alpha$ 1 and - $\alpha$ 2 isoforms in islets from mice with the indicated genotypes ( $n=3-4$ ) and **(b)** of *Ampk $\alpha$ 2* gene expression in hypothalamus (H), brain cortex (B), liver (L), spleen (S), kidney (K), muscle (M) and islet (I). cDNA generated by reverse transcription of extracted mRNA was analysed using primers targeting aa97–157 of AMPK $\alpha$ 1 and aa189–260 of AMPK $\alpha$ 2. For AMPK $\alpha$ 1, the product sizes were 588 and 408 bp for wild-type (Wt) and knockout alleles (null) respectively. The corresponding values for AMPK $\alpha$ 2 were 588 and 375 bp. **c** *Cre* mRNA levels in isolated islets and hypothalamic extracts and **(d)** analysis of deletion of *Ampk $\alpha$ 1* and *Ampk $\alpha$ 2* in

pancreatic islets. mRNA levels were quantified by qRT-PCR (see ESM 1). The indicated genotypes refer to the AMPK $\alpha$  isoform only. White bars, Wt; grey bars, heterozygous; black bars,  $\beta$ AMPKdKO. **e** Total AMPK activities in pancreatic islets from control (Ctrl; *Ampk $\alpha$ 1<sup>+/-</sup>,  $\alpha$ 2<sup>fl/fl</sup>, Cre<sup>-</sup>*), AMPK $\alpha$ 1 whole-body knockout ( $\alpha$ 1 KO; *Ampk $\alpha$ 1<sup>-/-</sup>,  $\alpha$ 2<sup>fl/fl</sup>, Cre<sup>-</sup>*),  $\beta$ AMPK $\alpha$ 2 KO ( $\alpha$ 2 KO; *Ampk $\alpha$ 1<sup>+/-</sup>,  $\alpha$ 2<sup>fl/fl</sup>, Cre<sup>+</sup>*) or  $\beta$ AMPKdKO (dKO; *Ampk $\alpha$ 1<sup>-/-</sup>,  $\alpha$ 2<sup>fl/fl</sup>, Cre<sup>+</sup>*) mice. **f** Body weight changes in  $\beta$ AMPKdKO (triangles) or control (circles; *Ampk $\alpha$ 1<sup>+/-</sup>,  $\alpha$ 2<sup>fl/fl</sup>, Cre<sup>+</sup>*) mice. **g** Food intake in fed mice (see Methods). Het, heterozygous. Data are expressed as means  $\pm$  SEM;  $n=3-5$  (**c**, **e**) or  $n=7-9$  (**f**, **g**); \* $p<0.05$ , \*\* $p<0.01$ , \*\*\* $p<0.001$

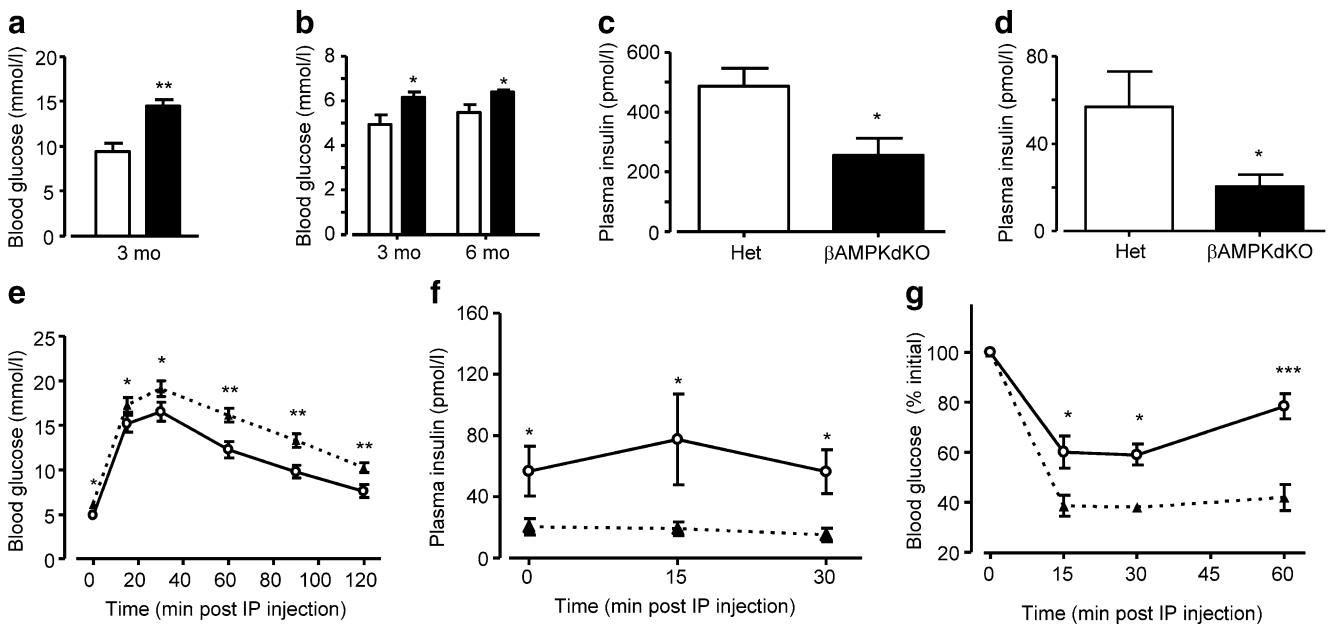


**Fig. 2** Glucose homeostasis in  $\beta$ AMPKdKO mice. Blood glucose (**a**, **b**) and plasma insulin (**c**, **d**) levels in 3- (**a**) or 3- and 6-month-old mice (**b**), or in 3-month old mice (**c**, **d**). For **b**, **c**, mice were fasted for 15 h. White bars, heterozygous (Het); black bars,  $\beta$ AMPKdKO. **e** Glucose tolerance

and **(f)** plasma insulin response, after intraperitoneal (IP) glucose injection, and **(g)** whole-body insulin sensitivity after IP insulin injection. Triangles,  $\beta$ AMPKdKO; circles, Het. Data are expressed as means  $\pm$  SEM;  $n=7-9$ ; \* $p<0.05$ , \*\* $p<0.01$ , \*\*\* $p<0.001$

measured from blood collected from tail veins of 12-week-old mice between 10:00 and 11:00 hours.

**Insulin tolerance test** Bovine insulin (0.75 U/kg; Sigma, Dorset, UK) was intraperitoneally injected into fed mice between 13:00 and 14:00 hours. Blood glucose levels were measured at 0, 15, 30 and 60 min after injection.

#### Urine collection and catecholamine measurement

Daily urine collection from each mouse for a period of 3 days was performed using metabolic cages. Catecholamine levels in urine were determined by reverse-phase HPLC.

#### Other methods

Details of islet isolation and insulin secretion, electron microscopy, electrophysiology, optical projection tomography,  $\text{Ca}^{2+}$  imaging, RNA extraction and RT-PCR, AMPK assay, antibodies and immunohistochemistry are provided in Electronic supplementary material (ESM 1).

#### Statistical analysis

Data are expressed as means  $\pm$  SEM. Significance was tested by two samples unpaired or paired Student's *t* test using Excel, or by ANOVA using Graphpad 4.0. A value of  $p < 0.05$  was considered significant.

## Results

$\beta$ AMPKdKO mice have normal body weight but are hyperglycaemic

mRNAs encoding *Ampk $\alpha$ 1* and  $-\alpha$ 2 subunits were present in highly purified [32, 33] wild-type mouse beta cells (ESM Fig. 1). *Ampk $\alpha$ 1* mRNA was ~15-fold more abundant than that encoding the  $\alpha$ 2 subunit, in line with previous AMPK activity measurements in clonal beta cells [5] and with the distinct roles of each isoform in these cells [5]. Since mice deleted globally for either subunit display essentially normal insulin release in vitro [13], we generated trigenic mice inactivated for AMPK $\alpha$ 1 and  $\alpha$ 2 subunits selectively in beta cells and in a small population of hypothalamic neurons. Mice globally inactivated for *Ampk $\alpha$ 1* [11] were first crossed with animals bearing floxed *Ampk $\alpha$ 2* gene alleles (Fig. 1a). Crossing with *RIP2.Cre* mice [29] led to a selective loss of the catalytic domain of the *Ampk $\alpha$ 2* subunit (aa189–260) from islets and hypothalamus (Fig. 1a, b). Consistent with the abundant expression in islets of the *Cre* transgene (Fig. 1c) and selective deletion of the two catalytic subunits

from beta cells [34], the crossing of *Ampk $\alpha$ 2* floxed and *RIP2.Cre* mice resulted in a decrease in islet *Ampk $\alpha$ 2* mRNA of 60 to 70% (Fig. 1d). Assessed at low glucose concentrations to near-maximally stimulate the enzyme [14], total islet AMPK activity was decreased by 93% in *Ampk $\alpha$ 1<sup>-/-</sup>* vs *Ampk $\alpha$ 1<sup>+/-</sup>* ( $\alpha$ 2<sup>fl/fl</sup>.*Cre*<sup>-</sup> in each case) mice and by 95% in  $\beta$ AMPKdKO mice vs *Ampk $\alpha$ 1<sup>+/-</sup>* (Fig. 1e).

Male  $\beta$ AMPKdKO mice displayed entirely normal growth and normal food intake (Fig. 1f, g), while females had a small reduction in body weight up to 10 weeks of age (ESM Fig. 2a). Assessed at 3 (Fig. 2a, c) and 6 months (not shown) of age,  $\beta$ AMPKdKO mice of either sex, but not mice deleted for either *Ampk $\alpha$ 1* [12] or  $-\alpha$ 2 (ESM Fig. 3) alone, displayed markedly elevated plasma glucose and decreased plasma insulin levels (Fig. 2a–d, ESM Fig. 3). Correspondingly, double knockout mice displayed abnormal glucose tolerance and insulin release in vivo, despite increased insulin sensitivity (Fig. 2e–g, ESM Fig. 2c–e). No differences in glucose tolerance and insulin release or sensitivity were observed between *Ampk $\alpha$ 1<sup>+/-</sup>*,  $\alpha$ 2<sup>+/-</sup>, *Cre*<sup>+</sup> and *Ampk $\alpha$ 1<sup>+/-</sup>*,  $\alpha$ 2<sup>fl/fl</sup>, *Cre*<sup>+</sup> control mice (not shown).

Since mice with global homozygous deletion of *Ampk $\alpha$ 2* display abnormal insulin secretion in vivo and elevated catecholamine levels [13], we determined whether the latter variable may contribute to abnormal insulin secretion in

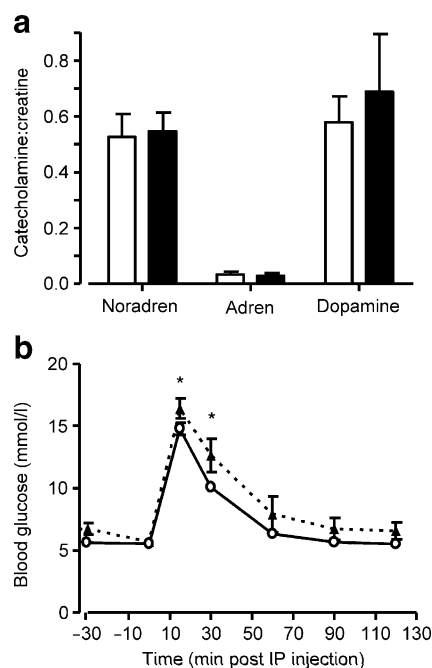


**Fig. 3** Role of catecholamines in the control of insulin secretion in  $\beta$ AMPKdKO mice. **a** Urinary noradrenaline (Noradren, norepinephrine), adrenaline (Adren, epinephrine) and dopamine levels. Black bars,  $\beta$ AMPKdKO; white bars, heterozygous. **b** Glucose tolerance of  $\beta$ AMPKdKO (triangles) or heterozygous control (white circles) mice 30 min. after IP phentolamine injection. Male mice aged 12–14 weeks were used. Data are expressed as means  $\pm$  SEM;  $n=6-8$ ; \* $p < 0.05$

$\beta$ AMPKdKO mice. We detected no alterations in the levels of urinary catecholamines (Fig. 3a), indicating that the above was not the case. Moreover, abnormal glucose tolerance was still observed, albeit diminished in extent, in the presence of the  $\alpha$ -adrenoreceptor blocker, phentolamine (Fig. 3b) [35].

$\beta$ AMPKdKO mice have normal beta cell mass but smaller beta cells and islets

Changes in relative beta cell mass, which might have explained the marked decrease in insulin release in  $\beta$ AMPKdKO animals, were not observed as assessed by optical projection tomography of whole pancreases [36] (Fig. 4a–d; ESM video clips 1 and 2) or through analysis of pancreatic slices (ESM Fig. 4). However, the distribution of islet sizes between heterozygous and  $\beta$ AMPKdKO animals, as assessed by optical projection tomography, revealed a significant  $\sim$ 40% decrease in the average volume of individual islets (Fig. 4b, c, e).

By contrast, no differences were apparent in the ratio of alpha to beta cells within individual islets or in the relative disposition of the two cell types (Fig. 5a). Similarly, despite proposed roles for AMPK and the upstream kinase liver

kinase B1 (LKB1) in the control of beta cell polarity [37–39] (G. Sun, A.I. Tarasov, J. McGinty, P.M. French, A. McDonald, I. Leclerc and G. Rutter, unpublished results), we observed no abnormalities in the formation of adherens (anti-E-cadherin antibodies; Fig. 5b) or tight (anti-zona occludins-1 [ZO-1] antibody) junctions (Fig. 5c), and microfilament and microtubule structure were unchanged in islets from  $\beta$ AMPKdKO mice (not shown).

AMPK is a known regulator of the mechanistic target of rapamycin (mTOR) complex, acting to phosphorylate the mTORC1 components Raptor and the upstream regulator tuberous sclerosis complex-2 [40]. Since mTOR is involved in the regulation of cell size [41], we assessed the size of individual beta cells, using anti-E-cadherin (Fig. 5d, e) or anti-GLUT2 (not shown) antibodies to label the plasma membrane. This revealed an  $\sim$ 18% decrease in the average area of beta cells, corresponding to a decrease in volume of  $\sim$ 36%, closely in line with the reduction in average islet size. However, no changes in the phosphorylation state of the downstream targets of mTOR, ribosomal S6 subunits, were detected (not shown), arguing against changes in the activity of the latter pathway being responsible for the decrease in beta cell volume. Unexpectedly, beta cell

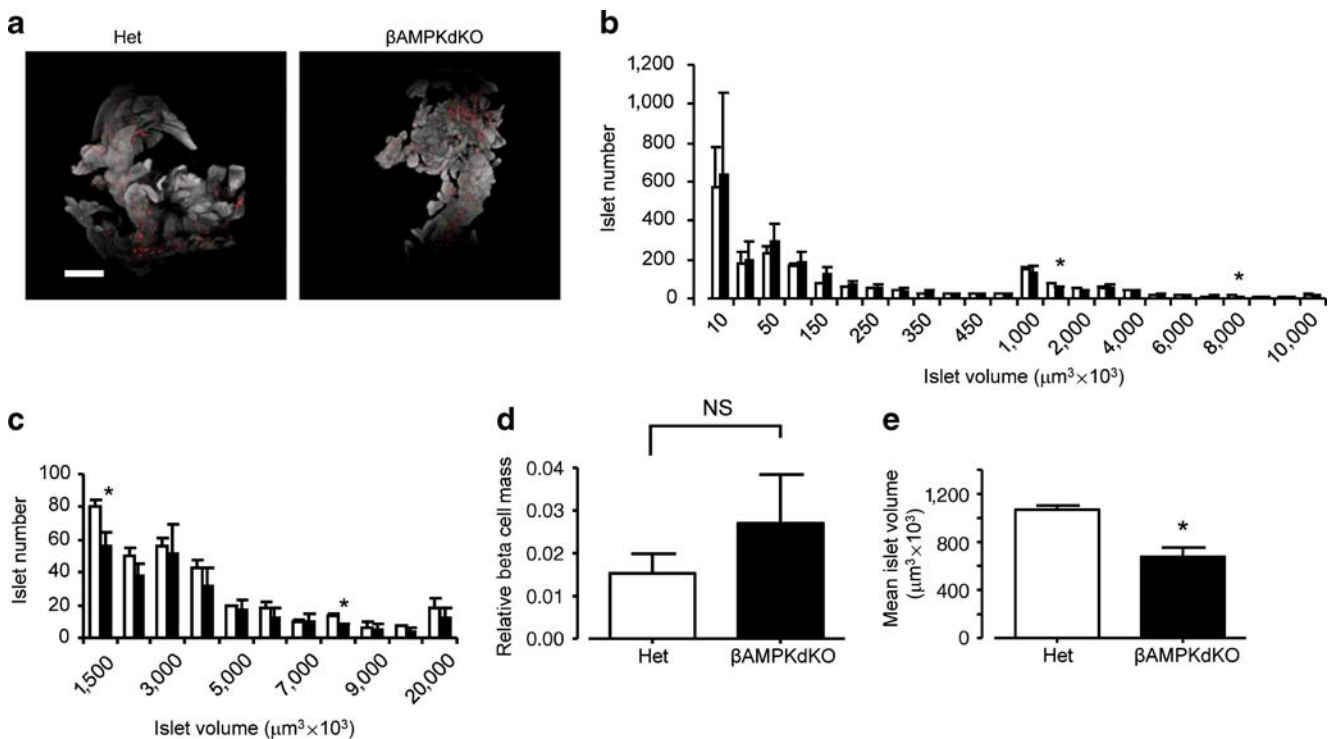


**Fig. 4**  $\beta$ AMPKdKO mice have normal beta cell mass but small islets and beta cells. **a** Representative optical projection tomographic projections of whole fixed and permeabilised pancreases. Optical projection tomography was performed as described in ESM. Red, insulin-positive structures (beta cells within islets). The overall shape of the whole pancreas was visualised as autofluorescence and is apparent as white/grey shading. The images shown correspond to

three dimensional projections; see also ESM clips 1 and 2. Het, heterozygous. Scale bar, 500  $\mu$ m. **b** Distribution of islet volumes with marked (dotted lines) section magnified (c). Black bars,  $\beta$ AMPKdKO; white bars, heterozygous. **d** Relative beta cell mass and (e) mean islet volume. Data are from  $n=3$  whole mouse pancreases per genotype and are expressed as means  $\pm$  SEM; \* $p<0.05$

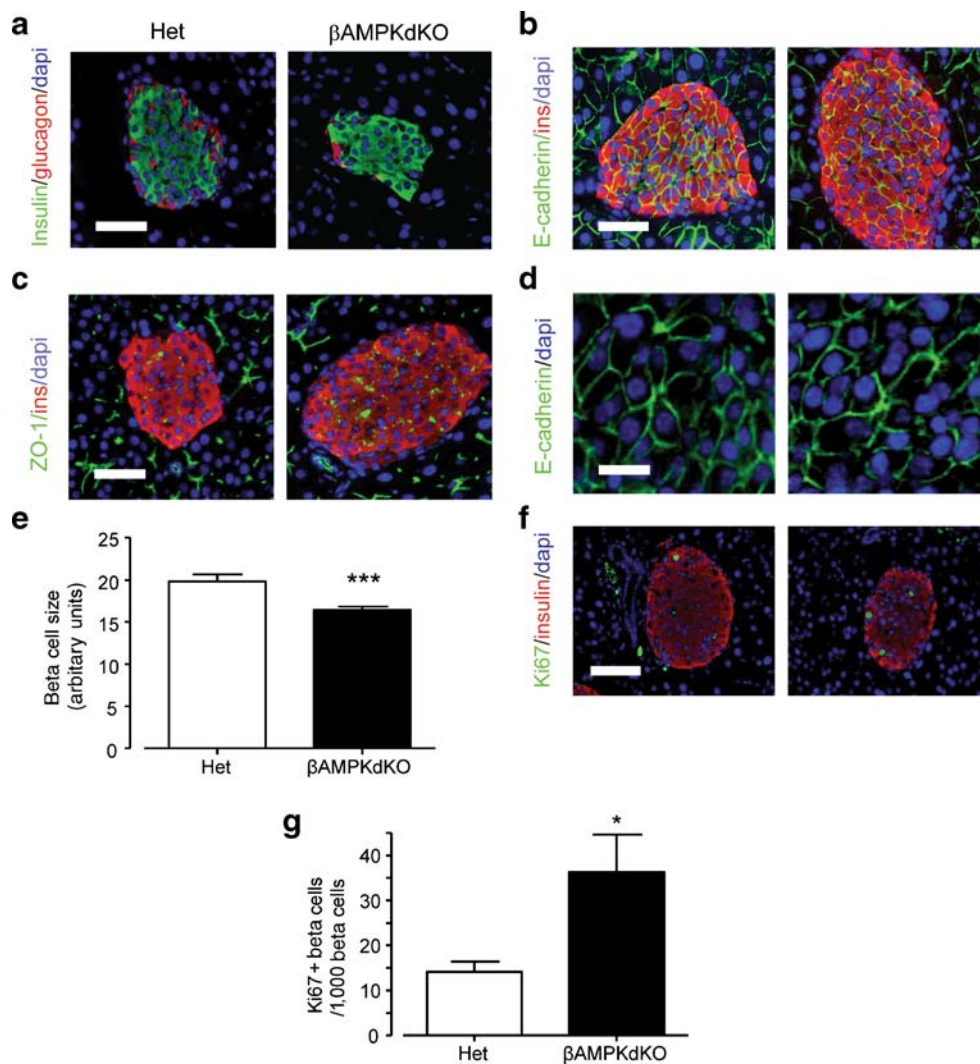


**Fig. 5** Islet and beta cell morphology in  $\beta$ AMPKdKO mice. Immunofluorescence staining of pancreatic sections with: (a) anti-insulin (1:200; red) and glucagon (1:100, green) antibodies; (b) the adherens junction marker E-cadherin (1:100; green); (c) tight junction marker ZO-1 (whole serum; green); and (d) representative E-cadherin staining of pancreatic sections and determination (e) of beta cell size

(see ESM 1). Ten islets (containing  $\geq 10$  cells) from  $n=3$  mice of each genotype were analysed. **f** Staining for proliferation marker Ki67 and quantification (g), based on 8–10 islets per pancreas,  $n=3$  per genotype. Scale bars: 75  $\mu$ m (a–c, f), 12  $\mu$ m (d). Data are expressed as means  $\pm$  SEM; \* $p < 0.05$ , \*\*\* $p < 0.001$

proliferation was also substantially (more than twofold) increased, as assessed by Ki67 staining (Fig. 5f, g). No changes in the low level of apoptosis could be detected by caspase-3 or in situ TUNEL staining (not shown), possibly reflecting rapid clearance of apoptotic cells.

Glucose-induced insulin secretion is enhanced in islets from  $\beta$ AMPKdKO mice but beta cell electrical activity and intracellular free  $\text{Ca}^{2+}$  changes are normal

The above analyses revealed a profound compromise in the capacity of an unchanged mass of morphologically normal beta cells to release insulin in vivo. To determine whether this reflected a change in the intrinsic properties of beta

cells, we next analysed insulin release from isolated islets and glucose-sensing by dissociated beta cells. In contrast to what was observed in vivo, islets from  $\beta$ AMPKdKO mice displayed significantly elevated rates of glucose-stimulated insulin release compared with control (heterozygote) islets (Fig. 6a), arguing for a restraining effect of AMPK on hormone release. Unexpectedly, the previously described inhibitory effects of AMPK activation with the AMPK activator and AMP analogue AICAR [4, 6] were still preserved in  $\beta$ AMPKdKO mouse islets, indicating that the effects of this activator were largely independent of AMPK.

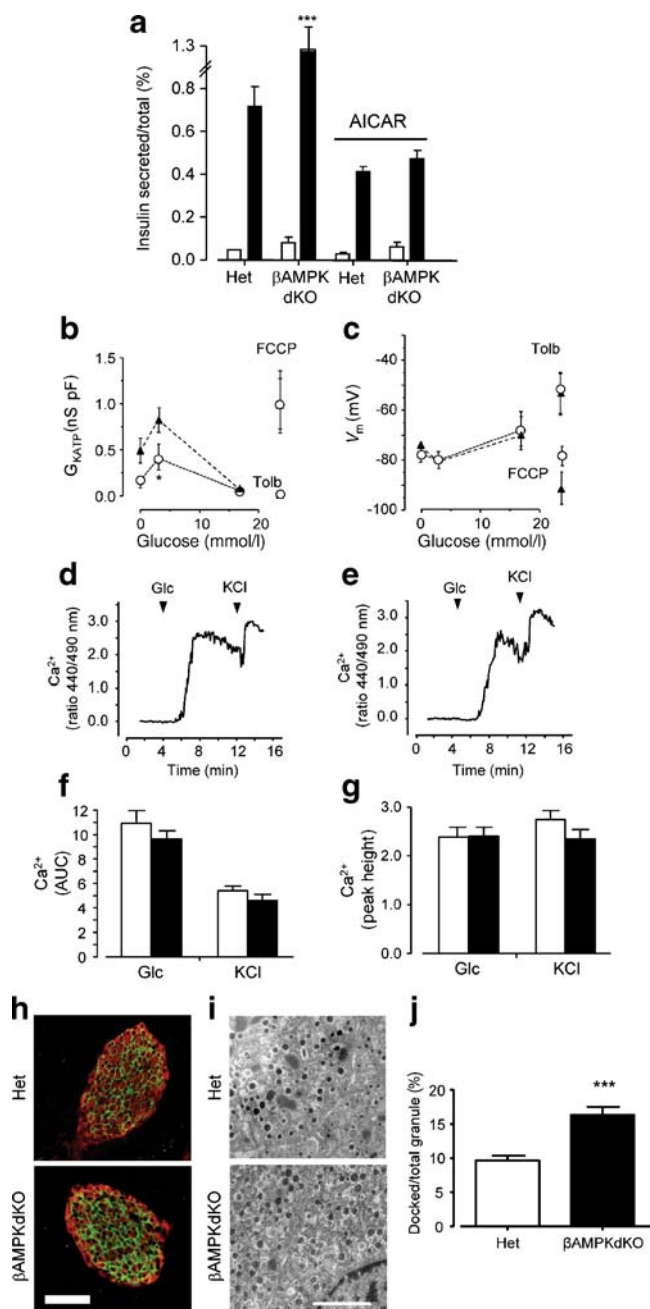
To determine whether beta cells from  $\beta$ AMPKdKO mouse islets show altered glucose sensing, as observed after LKB1 deletion (G. Sun, A. Tarasov, J. McGinty, P.M. French, A.

McDonald, I. Leclerc and G. Rutter, unpublished results), we used electrophysiological approaches. While glucose-induced changes in the conductance of ATP-sensitive  $K^+$  channels revealed lower conductance of these channels at low (3 mmol/l) but not elevated (16.7 mmol/l) glucose in  $\beta$ AMPKdKO beta cells compared with heterozygous controls, this did not translate into a difference in membrane potential changes (Fig. 6b, c). Likewise, no differences were apparent in the extent of glucose or depolarisation- (KCl-) induced increases in intracellular free  $Ca^{2+}$  ions in heterozygous compared with  $\beta$ AMPKdKO beta cells (Fig. 6d–g). Correspondingly, again in contrast to the impact of LKB1 deletion (G. Sun, A. Tarasov, J. McGinty, P.M. French, A. McDonald, I. Leclerc and G. Rutter, unpublished results), no differences were observed in the levels or plasma membrane association of the liver/beta cell glucose transporter Glut2 (Fig. 6h) [42]. By contrast, the number of morphologically docked granules was significantly increased in  $\beta$ AMPKdKO beta cells (Fig. 6i, j).

We next determined whether AMPK present in beta cells and *RIP2.Cre* neurons contribute to the deleterious effects of a high-fat diet on insulin release and glucose homeostasis [43]. No differences in body weight gain were apparent between heterozygous and  $\beta$ AMPKdKO mice maintained on high-fat diet (Fig. 7a). However, after 6 weeks on high-fat diet, which is sufficient to cause profound abnormalities in glucose-induced insulin secretion in C57BL/6 mice [43], the differences in glycaemia observed between heterozygote and  $\beta$ AMPKdKO mice observed on a normal diet

(Fig. 2a, b, e) were abolished (Fig. 7b). This change reflected a more dramatic increase in glucose levels in the heterozygous mice on high-fat diet than in those on normal chow (Figs 2a and 7b). Likewise, the difference in glucose tolerance observed between  $\beta$ AMPKdKO and heterozygous mice on normal chow (~5 mmol/l at 60 min; Fig. 2e) was substantially reduced when the comparison between genotypes was performed in mice maintained on high-fat diet (~2 mmol/l at 60 min; Fig. 7c). By contrast, the enhanced insulin sensitivity of  $\beta$ AMPKdKO mice (~20% of the initial glucose level 30 min. post insulin injection; Fig. 2g) was maintained or enhanced on high-fat diet

**Fig. 6** Unaltered glucose-induced changes in membrane potential and intracellular free  $Ca^{2+}$  in  $\beta$ AMPKdKO mouse beta cells, but enhanced granule docking and improved glucose-stimulated insulin secretion in isolated islets. **a** Glucose-stimulated insulin secretion of six size-matched islets from  $\beta$ AMPKdKO and heterozygous mice (Het) statically incubated with 3 mmol/l (white bars) or 16.7 mmol/l (black bars) glucose or 400  $\mu$ mol/l AICAR for 0.5 h;  $n=3$  per genotype. **b** Representative traces of whole-cell  $K_{ATP}$  channel conductance ( $G_{KATP}$ ) and plasma membrane potential ( $V_m$ ) (**c**) from perforated patch clamp. Six to nine cells from three mice of each genotype were analysed. nS pF, nanosiemens picofarad; FCCP, carbonyl cyanide-*p*-trifluoromethoxyphenylhydrazone; Tolb, tolbutamide; triangles, *Ampk $\alpha$ 1<sup>+/+</sup>*; circles, *Ampk $\alpha$ 1<sup>-/-</sup>*; **d** Representative traces of free [ $Ca^{2+}$ ] with fura-red in dissociated beta cells in heterozygous and (**e**)  $\beta$ AMPKdKO mice, with quantification (**f** [AUC in arbitrary fluorescent units], **g**); 19–22 cells from two mice of each genotype were analysed. Glc, glucose; white bars, heterozygous; black bars,  $\beta$ AMPKdKO. **h** Immunofluorescence staining of GLUT2 expression at the plasma membrane of pancreatic islet beta cells; 15 islets from two pairs of mice of each genotype were analysed. Scale bar, 75  $\mu$ m. Het, heterozygous. **i** Granule docking in control (Het) or  $\beta$ AMPKdKO beta cells; 15 cells from four separate islets, two mice per genotype were analysed by transmission electron microscopy. The relative number of morphologically docked granules was calculated by dividing that of docked granules (those within 400 nm of the plasma membrane) by that of total cytosolic granule number and is quantified in bar graph (**j**), see ESM 1. Scale bar, 2  $\mu$ m. Data are expressed as means  $\pm$  SEM; \*\*\* $p<0.001$





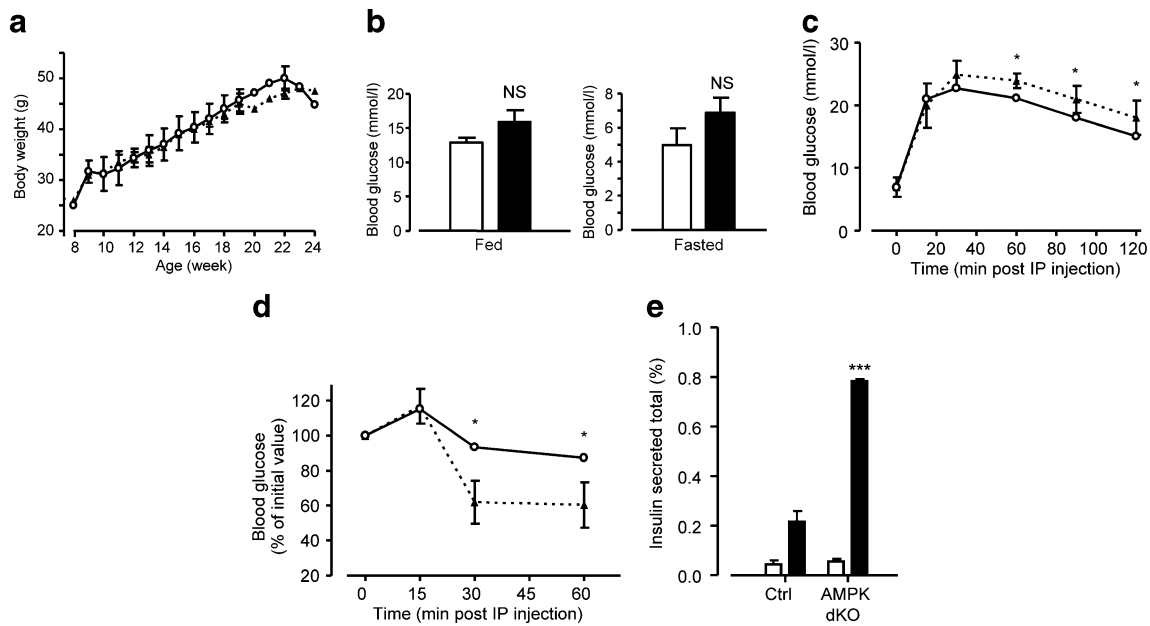


**Fig. 7** AMPK deletion attenuates the deleterious effects of high-fat feeding on glucose tolerance. **a** Body weight changes in  $\beta$ AMPKdKO (triangles) and heterozygous (circles) mice over 2 to 18 weeks on high-fat diet (60%). **b** Blood glucose levels in  $\beta$ AMPKdKO (black bars) and heterozygous (white bars) mice on high-fat diet for 6 weeks with free access to food or fasted for 15 h. **c** Glucose tolerance after intraperitoneal (IP) glucose injection and **(d)** whole-body insulin

sensitivity after IP insulin injection of  $\beta$ AMPKdKO mice on high-fat diet for 6 weeks. Triangles,  $\beta$ AMPKdKO; circles, heterozygous. **e** Glucose-stimulated insulin secretion of six size-matched islets from  $\beta$ AMPKdKO and control (Ctrl) mice maintained on high-fat diet for 18 weeks. Islets were statically incubated at 3 mmol/l (white bars) and 16.7 mmol/l (black bars) glucose for 0.5 h.  $n=3$  mice per each genotype. Data are expressed as means  $\pm$  SEM; \* $p<0.05$ , \*\*\* $p<0.001$

(~30% of initial glucose; Fig. 7d). Strikingly, the 3.5-fold decrease in glucose-stimulated insulin secretion observed in islets from heterozygous mice maintained on high-fat diet compared with normal chow (from ~0.7 to 0.2% per 30 min; Figs 6a and 7e) was reduced in  $\beta$ AMPKdKO mouse islets to ~0.6-fold (from ~1.3 to 0.8% per 30 min.). Hence,  $\beta$ AMPKdKO mice were still susceptible to the effects of high-fat diet, albeit to a lesser extent than controls.

Overexpression of constitutively active AMPK in beta cells causes glucose intolerance

The above results suggested that, at extrapancreatic sites of *RIP2.Cre* expression, notably in the mediobasal hypothalamus, AMPK activity is permissive of insulin secretion in vivo.

To determine whether increases in AMPK imposed selectively in beta cells affect insulin secretion in vivo, we generated transgenic mice in which the constitutively active enzyme (AMPK.CA) [6] was expressed under the control of the insulin promoter (Fig. 8a). Of two founder mouse lines generated (Fig. 8b), we examined in detail one line carrying two transgene copies. Overexpression of the mRNA was clearly evident in islets (Fig. 8c, d) and under the control of glucose ex vivo (as expected for expression under the insulin promoter; Fig. 8e), but barely (<0.001%

of the islet level) in the hypothalamus or other tissues (Fig. 8d, f), reflecting the more restricted expression of the *RIP2* transgene to the beta cell in adult mice [44].

Islets from transgenic mice overexpressing AMPK.CA (AMPK.CA transgenic) displayed a significant increase in total ( $\alpha 1 + \alpha 2$  complex) AMPK activity at elevated (16.7 mmol/l), but not at low (2.8 mmol/l) glucose concentrations, where the endogenous enzyme was strongly activated (Fig. 8g, h) [14]. Conversely, AMPK activity was reduced at low glucose concentrations in islets from AMPK.DN transgenic mice, generated in parallel with AMPK.CA mice (Fig. 8g, h). Assuming approximately equal endogenous AMPK levels in beta compared with islet non-beta cells (ESM Fig. 1) and an islet beta cell content of 60% [34], AMPK activity was increased by 36% and reduced by 50%, in beta cells by overexpression of AMPK.CA or AMPK.DN respectively.

Maintained on normal chow, AMPK.CA and AMPK.DN transgenic mice displayed normal body weight increases (Fig. 9a, b). Whereas male AMPK.CA transgenic mice displayed abnormal glucose tolerance at 3 (Fig. 9c), but not 6 (Fig. 9e) months, no abnormalities were seen in AMPK.DN transgenic animals (Fig. 9d, f) or in female AMPK.CA mice (not shown). The abnormalities in AMPK.CA transgenic mice were not associated with any alterations in insulin sensitivity (Fig. 9g, h), but with decreased fasting

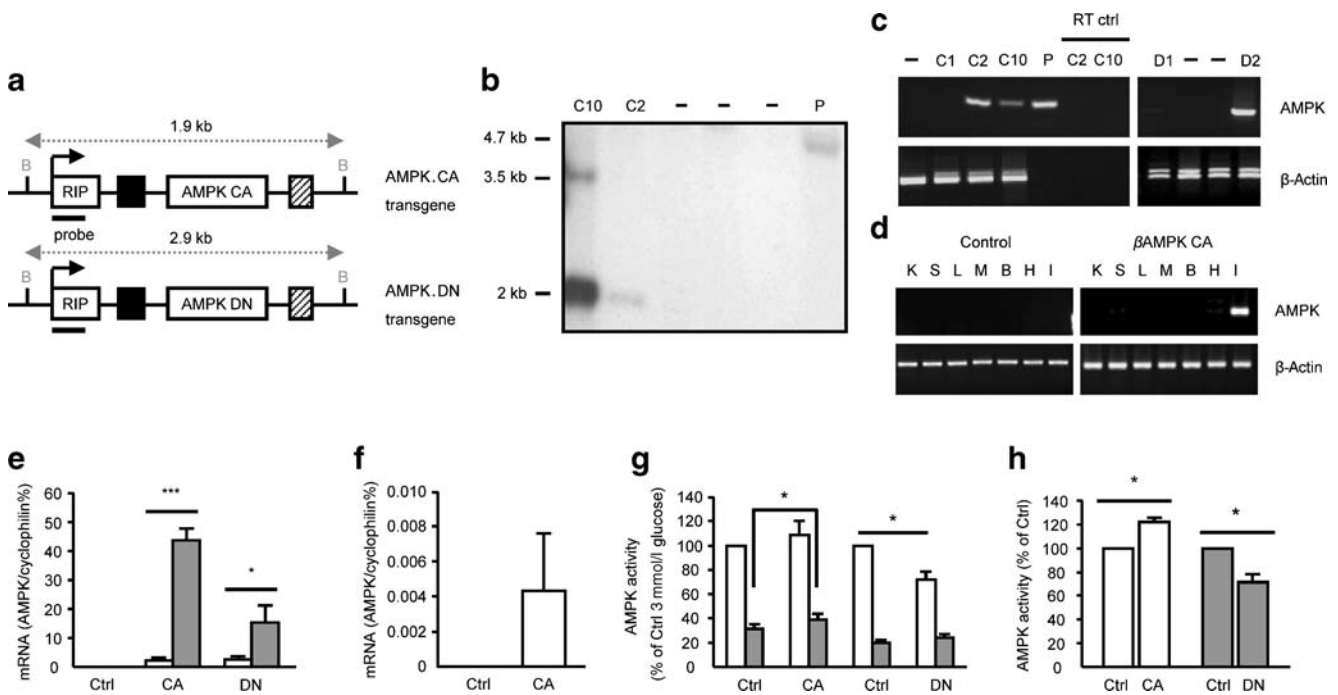


**Fig. 8** Generation of  $\beta$ AMPK.CA and  $\beta$ AMPK.DN transgenic mice. **a** Schematic representation (not to scale) of RIP2-AMPK.CA and DN constructs for generating the transgenic mice. Black square, *c-myc* sequence. Hatched square, poly A sequence. B, BssHIII digestion site. **b** Southern blot analysis of tail DNA from offspring of  $\beta$ AMPK.CA founder mice. Expected fragment sizes of RIP2-AMPK.CA constructs with linearisation of head-to-tail (1.9 kb) or of head-to-head (3.5 kb) in the mice genomic DNA after SpeI digestion and hybridisation with indicated probe situated in the RIP2 promoter are shown. P, two equivalent copies of RIP2-AMPK.CA vectors (4.7 kb). **c** RT-PCR analysis of AMPK transgene expression in islets and **(d)** hypothalamus (H), brain cortex (B), liver (L), spleen (S), kidney (K), muscle (M) and islet (I) from  $\beta$ AMPK transgenic mice and their wild-type

controls. C, AMPK.CA; D, AMPK.DN; dashed bar, wild-type; P, 5 ng AMPK.CA plasmid used for generating transgenic mice. **e** Quantification of real-time PCR analysis of AMPK transgene expression in islets and **(f)** hypothalamus from transgenic mice and their wild-type controls. Islets were incubated for 24 h at 3 mmol/l (white bars) or 16.7 mmol/l (grey bars) glucose before RNA extraction;  $n=3$  mice per genotype. RNA was extracted from hypothalamic extracts immediately after isolation. **g, h** Total AMPK activity in islets from transgenic mice and their wild-type littermate controls. Islets were incubated for 24 h at glucose concentrations as above (**e, f**) prior to extraction and assay (see ESM 1). Male mice aged from 12 to 14 weeks old were used;  $n=3-5$ . Results are from three or more independent experiments and are expressed as mean  $\pm$  SEM; \* $p<0.05$ , \*\*\* $p<0.001$

and stimulated plasma insulin levels (Fig. 9i, j) and a 25% decrease in beta cell area ( $0.09\pm 0.02\%$  in wild-type vs  $0.068\pm 0.04\%$  in transgenic littermates; data not shown). No significant changes in these variables were observed in AMPK.DN transgenic mice.

To determine whether the alterations in insulin secretion in AMPK.CA mice also result from defects at the level of the beta cell, we performed studies with isolated islets. Insulin release stimulated by 16.7 mmol/l glucose was decreased by >60% (Fig. 9k), a similar change to that observed after maintenance of mice for 18 weeks on high-fat diet. Indeed, islets from AMPK.CA transgenic mice maintained on high-fat diet displayed no further diminution in glucose-stimulated insulin secretion compared with wild-type littermates on the same diet (Fig. 9k). Conversely, glucose-stimulated insulin release was significantly enhanced in islets from AMPK.DN transgenic mice (Fig. 9l), reminiscent of the effect of deleting AMPK $\alpha 1$  and  $\alpha 2$  subunits (Fig. 6a), although in this case the improved secretion was eliminated in islets from animals fed a high-fat diet.

## Discussion

The principal aim of this study was to determine the physiological impact of complete and selective loss of both catalytic isoforms of AMPK from pancreatic beta cells. This is an important question, given the likely role of AMPK as a target for glucose-lowering drugs and uncertainties surrounding the role of AMPK in the beta cell [5, 6, 15, 18, 21, 45, 46].

### Cell autonomous roles of AMPK within the beta cell

Examined here in isolated islets and beta cells, total inactivation of AMPK led to a potentiation of glucose-induced insulin secretion. We also noted an increase in ATP-sensitive K<sup>+</sup> (K<sub>ATP</sub>) channel activity at low glucose concentrations (Fig. 4b, c), perhaps reflecting altered trafficking of channel subunits [47]. However, glucose-induced K<sub>ATP</sub> channel closure and increases in intracellular Ca<sup>2+</sup> were unaltered, suggesting that the loss of an

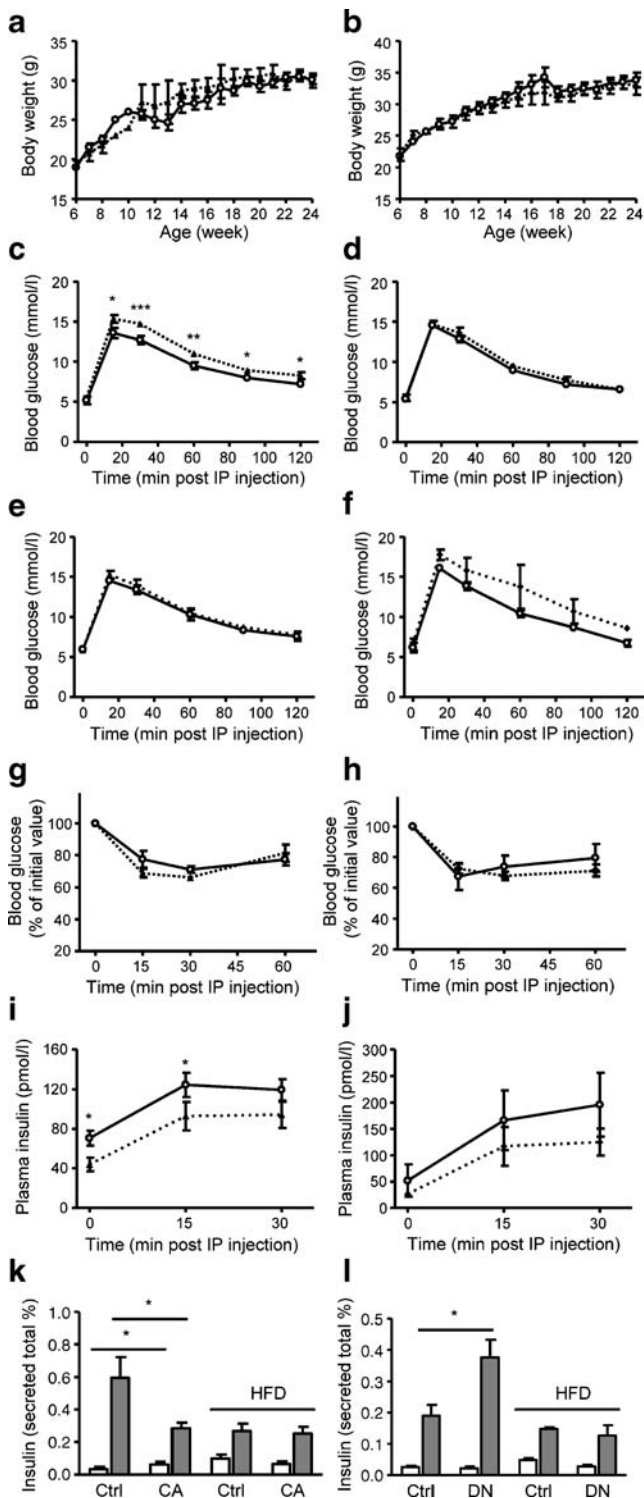


**Fig. 9**  $\beta$ AMPK.CA transgenic mice display mild glucose intolerance and reduced insulin secretion. **a** Growth curves of body weights of AMPK.CA mice and **(b)** AMPK.DN mice aged 6 to 24 weeks old. **c** Glucose tolerance at 3 months in AMPK.CA and **(d)** AMPK.DN mice, and **(e, f)** at 6 months respectively. **g** Whole-body insulin sensitivity in AMPK.CA and **(h)** AMPK.DN mice, with **(i, j)** insulin response of respective 3-month-old mice assessed by intraperitoneal (IP) injection and measurements of glucose in tail vein at the indicated times (see the Methods). White symbols (**a–j**),  $\beta$ AMPK.CA or  $\beta$ AMPK.DN; black symbols, control. **k** Glucose-stimulated insulin secretion assessed in islets from  $\beta$ AMPK.CA and **(l)**  $\beta$ AMPK.DN transgenic mice and their wild-type littermate controls on normal chow or high-fat (60%) diet (under the bar below HFD) for 18 weeks. Male mice aged 12–14 weeks were used;  $n=8–13$  (**a–j**),  $n=3–5$  (**k, l**). Data are expressed as means  $\pm$  SEM; \* $p<0.05$ , \*\* $p<0.01$ , \*\*\* $p<0.001$

overexpression in islets from of AMPK.CA animals in vitro [21], as well as with the effects of pharmacological activation of AMPK in clonal beta cells and isolated islets using AICAR or metformin [4, 6, 14, 48]. Furthermore, a diminished number of docked granules was observed in MIN6 cells overexpressing AMPK.CA [16].

We also show here that AMPK deletion leads to a decrease in cell volume, an effect strikingly different from that of deleting the upstream kinase, LKB1. Indeed, beta cells lacking LKB1 as a result of excision mediated either by *RIP2.Cre* (G. Sun, A. Tarasov, J. McGinty) or pancreas duodenum homeobox-1 promoter/Cre recombinase-oestrogen receptor (PDX-1-CreER) [38, 49] are larger than wild-type beta cells. LKB1 and AMPK appear therefore to engage substantially distinct downstream signalling pathways in beta cells, the former acting at least to a large extent via polarity-regulating kinase partitioning-defective 1/microtubule affinity-regulating kinase 2 (PAR1B/MARK2) [38, 49].

In the present study, inactivation of AMPK in *RIP2.Cre* neurons exerted no apparent effect on body mass or food intake. However,  $\alpha$ AMPKdKO mice displayed defective glucose homeostasis due to abnormalities in the capacity of a preserved beta cell mass to secrete insulin in response to hyperglycaemia. This deficiency was only partially compensated for by an increase in insulin sensitivity, probably due to increased insulin receptor levels or enhanced downstream signalling in target tissues [50]. Importantly, we used intraperitoneal injection of glucose, rather than oral administration to achieve increases in blood glucose concentration in the absence of a substantial release of incretins including glucagon-like peptide-1. In this way, we sought to compare the effects of an increase in circulating glucose in vivo with changes imposed on isolated islets. Nonetheless, we noted a dramatic decrease in insulin release in  $\beta$ AMPK.dKO mice in vivo, which was not apparent in vitro.

We considered the possibility that decreases in beta cell and islet size contribute to this deficiency in insulin secretion in vivo. However, the absence of impaired insulin release from islets in vitro (in fact, the opposite was

inhibitory effect of AMPK-mediated phosphorylation of kinesin light chains [16, 17] and increased granule translocation to the plasma membrane (Fig. 6i, j) may underlie the enhanced secretion. Conversely, selective activation of AMPK in beta cells in  $\beta$ AMPK.CA transgenic mice decreased glucose-stimulated insulin secretion. These findings are consistent with previous results involving the

observed) makes it unlikely that these changes are responsible for the drastically impaired insulin release observed in vivo in  $\beta$ AMPKdKO mice. It seems that the absence of the ‘opposite’ in vivo phenotype (i.e. improved glucose intolerance) in mice overexpressing activated AMPK under the same promoter (Fig. 9c, e, g, i) is most likely to reflect the predominant expression of the transgene in the pancreatic beta cell (rather than the hypothalamus) in adult mice. One possible explanation for these data is that a signal or signals emanating from *RIP2.Cre* neurons controls the activity of beta cells in vivo. Indeed, central administration of leptin has previously been shown to inhibit insulin secretion in vivo [51] and it is conceivable that this involves *RIP2.Cre* neurons and intracellular signaling pathways modulated by AMPK. Nevertheless, further and more definitive studies are needed to ascertain whether and by what means *RIP.Cre* neurons may influence insulin secretion.

A further interesting finding of the present studies is that mice lacking AMPK in the beta cell are somewhat less susceptible to the deleterious effects of high-fat diet on glucose metabolism and insulin secretion in vitro. These results are consistent with the previously demonstrated role of AMPK [18] in the actions of cytokines [19] on beta cell function and mass.

## Conclusions

The results presented here suggest that activation of AMPK in hypothalamic neurons and in pancreatic beta cells play distinct roles in the control of insulin release in vivo. Our findings should inform the use and development of agents that act through AMPK to control glycaemia.

**Acknowledgements** This work was supported by grants to G. A. Rutter from the Wellcome Trust (Programme Grant 081958/2/07/Z), The European Union (FP6 “Save Beta”), the Medical Research Council (G0401641) and National Institutes of Health (RO1 DK071962-01), as well as by a JDRFI Post-Doctoral Fellowship to A. I. Tarasov. We thank B. Kola (Queen Mary, University of London) for useful discussion, and P. Meda (University of Geneva) and B. Thorens (University of Lausanne) respectively for the kind provision of anti-ZO-1 and anti-GLUT2 antibodies. L. Lawrence is thanked for the preparation of pancreatic slices.

**Duality of interest** The authors declare that there is no duality of interest associated with this manuscript.

## References

- Shaw RJ, Lamia KA, Vasquez D et al (2005) The kinase LKB1 mediates glucose homeostasis in liver and therapeutic effects of metformin. *Science* 310:1642–1646
- Towler MC, Hardie DG (2007) AMP-activated protein kinase in metabolic control and insulin signaling. *Circ Res* 100:328–341
- Kurth-Kraczek EJ, Hirshman MF, Goodyear LJ, Winder WW (1999) 5' AMP-activated protein kinase activation causes GLUT4 translocation in skeletal muscle. *Diabetes* 48:1667–1671
- Salt IP, Johnson G, Ashcroft SJ, Hardie DG (1998) AMP-activated protein kinase is activated by low glucose in cell lines derived from pancreatic beta cells, and may regulate insulin release. *Biochem J* 335:533–539
- da Silva XG, Leclerc I, Salt IP et al (2000) Role of AMP-activated protein kinase in the regulation by glucose of islet beta-cell gene expression. *Proc Natl Acad Sci U S A* 97:4023–4028
- da Silva XG, Leclerc I, Varadi A, Tsuboi T, Moule SK, Rutter GA (2003) Role for AMP-activated protein kinase in glucose-stimulated insulin secretion and preproinsulin gene expression. *Biochem J* 371:761–774
- Rutter GA, Leclerc I (2009) The AMP-regulated kinase family: Enigmatic targets for diabetes therapy. *Mol Cell Endocrinol* 297:41–49
- Long YC, Zierath JR (2006) AMP-activated protein kinase signaling in metabolic regulation. *J Clin Invest* 116:1776–1783
- Stapleton D, Woollatt E, Mitchelhill KI et al (1997) AMP-activated protein kinase isoenzyme family: subunit structure and chromosomal location. *FEBS Lett* 409:452–456
- Hardie DG, Carling D (1997) The AMP-activated protein kinase—fuel gauge of the mammalian cell? *Eur J Biochem* 246: 259–273
- Viollet B, Andreelli F, Jorgensen SB et al (2003) Physiological role of AMP-activated protein kinase (AMPK): insights from knockout mouse models. *Biochem Soc Trans* 31:216–219
- Jorgensen SB, Viollet B, Andreelli F et al (2004) Knockout of the  $\alpha 2$  but not  $\alpha 1$  5'-AMP-activated protein kinase isoform abolishes 5-aminoimidazole-4-carboxamide-1- $\beta$ -D-ribofuranoside but not contraction-induced glucose uptake in skeletal muscle. *J Biol Chem* 279:1070–1079
- Viollet B, Andreelli F, Jorgensen SB et al (2003) The AMP-activated protein kinase  $\alpha 2$  catalytic subunit controls whole-body insulin sensitivity. *J Clin Invest* 111:91–98
- Leclerc I, Woltersdorf WW, da Silva XG et al (2004) Metformin, but not leptin, regulates AMP-activated protein kinase in pancreatic islets: impact on glucose-stimulated insulin secretion. *Am J Physiol Endocrinol Metab* 286:E1023–E1031
- Richards SK, Parton LE, Leclerc I, Rutter GA, Smith RM (2006) Over-expression of AMP-activated protein kinase impairs pancreatic beta-cell function in vivo. *J Endocrinol* 187:225–235
- Tsuboi T, da Silva XG, Leclerc I, Rutter GA (2003) 5' AMP-activated protein kinase controls insulin-containing secretory vesicle dynamics. *J Biol Chem* 278:52042–52051
- McDonald A, Fogarty S, Leclerc I, Hill E, Hardie DG, Rutter GA (2009) Control of insulin granule dynamics by AMPK-dependent KLC1 phosphorylation. *Islets* 1:1–11
- Kefas BA, Heimberg H, Vaulont S et al (2003) AICA-riboside induces apoptosis of pancreatic beta cells through stimulation of AMP-activated protein kinase. *Diabetologia* 46: 250–254
- Riboulet-Chavey A, Diraison F, Siew LK, Wong FS, Rutter GA (2008) Inhibition of AMP-activated protein kinase protects pancreatic  $\beta$ -cells from cytokine-mediated apoptosis and CD8<sup>+</sup> T cell-induced cytotoxicity. *Diabetes* 57:415–423
- Jones RG, Plas DR, Kubek S et al (2005) AMP-activated protein kinase induces a p53-dependent metabolic checkpoint. *Mol Cell* 18:283–293
- Gleason CE, Lu D, Witters LA, Newgard CB, Birnbaum MJ (2007) The role of AMPK and mTOR in nutrient sensing in pancreatic beta-cells. *J Biol Chem* 282:10341–10351

22. Minokoshi Y, Alquier T, Furukawa N et al (2004) AMP-kinase regulates food intake by responding to hormonal and nutrient signals in the hypothalamus. *Nature* 428:569–574
23. McCrimmon RJ, Fan X, Cheng H et al (2006) Activation of AMP-activated protein kinase within the ventromedial hypothalamus amplifies counterregulatory hormone responses in rats with defective counterregulation. *Diabetes* 55:1755–1760
24. McCrimmon RJ, Shaw M, Fan X et al (2008) Key role for AMP-activated protein kinase in the ventromedial hypothalamus in regulating counterregulatory hormone responses to acute hypoglycemia. *Diabetes* 57:444–450
25. Claret M, Smith MA, Batterham RL et al (2007) AMPK is essential for energy homeostasis regulation and glucose sensing by POMC and AgRP neurons. *J Clin Invest* 117:2325–2336
26. Mountjoy PD, Bailey SJ, Rutter GA (2007) Inhibition by glucose or leptin of neuropeptide Y-expressing hypothalamic neurons requires changes in AMP-activated protein kinase activity. *Diabetologia* 50:168–177
27. Canabal DD, Song Z, Potian JG, Beuve A, McArdle JJ, Routh VH (2006) Glucose, insulin and leptin signaling pathways modulate nitric oxide (NO) synthesis in glucose-inhibited (GI) neurons in the ventromedial hypothalamus (VMH). *Am J Physiol Regul Integr Comp Physiol* 292:R1418–R1428
28. Wyatt CN, Mustard KJ, Pearson SA et al (2007) AMP-activated protein kinase mediates carotid body excitation by hypoxia. *J Biol Chem* 282:8092–8098
29. Choudhury AI, Heffron H, Smith MA et al (2005) The role of insulin receptor substrate 2 in hypothalamic and beta cell function. *J Clin Invest* 115:940–950
30. Lee JY, Ristow M, Lin X, White MF, Magnuson MA, Hennighausen L (2006) RIP-Cre revisited, evidence for impairments of pancreatic beta-cell function. *J Biol Chem* 281:2649–2653
31. Pomplun D, Florian S, Schulz T, Pfeiffer AF, Ristow M (2007) Alterations of pancreatic beta-cell mass and islet number due to Ins2-controlled expression of Cre recombinase: RIP-Cre revisited; part 2. *Horm Metab Res* 39:336–340
32. Reimann F, Habib AM, Tolhurst G, Parker HE, Rogers GJ, Gribble FM (2008) Glucose-sensing in L-cells: a primary cell study. *Cell Metabolism* 8:532–539
33. Nicolson TJ, Bellomo EA, Wijesekara N et al (2009) Insulin storage and glucose homeostasis in mice null for the granule zinc transporter ZnT8 and studies of the type 2 diabetes-associated variants. *Diabetes* 58:2070–2083
34. Rahier J, Goebbels RM, Henquin JC (1983) Cellular composition of the human diabetic pancreas. *Diabetologia* 24:366–371
35. Cerasi E, Effendic S, Luft R (1969) Role of adrenergic receptors in glucose-induced insulin secretion in man. *Lancet* 2:301–302
36. Alanentalo T, Asayesh A, Morrison H et al (2007) Tomographic molecular imaging and 3D quantification within adult mouse organs. *Nat Methods* 4:31–33
37. Williams T, Brenman JE (2008) LKB1 and AMPK in cell polarity and division. *Trends Cell Biol* 18:193–198
38. Fu A, Ng AC, Depatie C et al (2009) Loss of Lkb1 in adult beta cells increases beta cell mass and enhances glucose tolerance in mice. *Cell Metab* 10:285–295
39. Granot Z, Swisa A, Magenheim J et al (2009) LKB1 regulates pancreatic beta cell size, polarity, and function. *Cell Metab* 10:296–308
40. Shaw RJ (2009) LKB1 and AMP-activated protein kinase control of mTOR signalling and growth. *Acta Physiol (Oxf)* 196:65–80
41. Fingar DC, Salama S, Tsou C, Harlow E, Blenis J (2002) Mammalian cell size is controlled by mTOR and its downstream targets S6K1 and 4EBP1/eIF4E. *Genes Dev* 16:1472–1487
42. Thorens B, Sarkar HK, Kaback HR, Lodish HF (1988) Cloning and functional expression in bacteria of a novel glucose transporter present in liver intestine kidney and B-pancreatic islet cells. *Cell* 55:281–290
43. Ahren B, Simonsson E, Scheurink AJ, Mulder H, Myrsen U, Sundler F (1997) Dissociated insulinotropic sensitivity to glucose and carbachol in high-fat diet-induced insulin resistance in C57BL/6J mice. *Metabolism* 46:97–106
44. Gannon M, Shiota C, Postic C, Wright CVE, Magnuson M (2000) Analysis of the Cre-mediated recombination driven by rat insulin promoter in embryonic and adult mouse pancreas. *Genesis* 26:139–142
45. Kefas BA, Cai Y, Ling Z et al (2003) AMP-activated protein kinase can induce apoptosis of insulin-producing MIN6 cells through stimulation of c-Jun-N-terminal kinase. *J Mol Endocrinol* 30:151–161
46. Kefas BA, Cai Y, Kerckhofs K et al (2004) Metformin-induced stimulation of AMP-activated protein kinase in b-cells impairs their glucose-responsiveness and can lead to apoptosis. *Biochem Pharmacol* 68:409–416
47. Lim A, Park SH, Sohn JW et al (2009) Glucose deprivation regulates KATP channel trafficking via AMP-activated protein kinase (AMPK) in pancreatic  $\beta$ -cells. *Diabetes* 58:2813–2819
48. Targonsky ED, Dai F, Koshkin V et al (2006) alpha-lipoic acid regulates AMP-activated protein kinase and inhibits insulin secretion from beta cells. *Diabetologia* 49:1587–1598
49. Hezel AF, Gurumurthy S, Granot Z et al (2008) Pancreatic LKB1 deletion leads to acinar polarity defects and cystic neoplasms. *Mol Cell Biol* 28:2414–2425
50. Buren J, Liu HX, Lauritz J, Eriksson JW (2003) High glucose and insulin in combination cause insulin receptor substrate-1 and -2 depletion and protein kinase B desensitisation in primary cultured rat adipocytes: possible implications for insulin resistance in type 2 diabetes. *Eur J Endocrinol* 148:157–167
51. Kalra SP (2008) Disruption in the leptin-NPY link underlies the pandemic of diabetes and metabolic syndrome: new therapeutic approaches. *Nutrition* 24:820–826